JOURNAL OF MATERIALS SCIENCE 19 (1984) 1321–1332

Effect of strain, strain rate and temperature on cavity size distribution in a superplastic copper-base alloy

N. RIDLEY, D. W. LIVESEY
University of Manchester/UMIST Department of Metallurgy and Materials Science, Grosvenor Street, Manchester M1 7HS, UK

A. K. MUKHERJEE
Division of Materials Science and Engineering, Department of Mechanical Engineering, University of California, Davis, CA 95616, USA

The distribution of cavity sizes in a microduplex α/β copper–zinc–nickel–manganese alloy (a nickel-silver) subjected to superplastic tensile straining has been examined as a function of strain, temperature and strain rate using quantitative optical metallography. The number of cavities that became optically visible increased throughout straining, but the rate at which they became visible decreased at higher strains. The distributions of cavity sizes in specimens deformed to the same strain at different temperatures or strain rates were essentially identical. The size distribution data were fully consistent with the observations that for a given strain the overall volume of cavities formed in the alloy was independent of temperature and strain rate. Growth for all cavity sizes is dominated by matrix plastic flow. The insensitivity of void volume and cavity size distribution to strain rate and temperature, and hence stress, reflects the resolution of the density and metallographic techniques. While higher stresses will lead to a wider range of initial cavity sizes by lowering the critical nucleus size, cavities at the lower end of the size range will not grow sufficiently to become optically resolvable or to produce a density differential compared with a specimen deformed to the same extent at a lower stress.

1. Introduction

It is well established for copper-base alloys that during superplastic tensile flow [1–8] cavitation occurs at grain boundaries. Work on microduplex α/β brasses has shown that the level of cavitation for a given strain increases as the proportion of α-phase in the microstructure increases, [3, 5, 6] while fine grain superplastic α-phase alloys are particularly prone to cavitation [4, 8]. For alloys containing a high volume fraction of α-phase, or alloys which are fully α-phase, it has been observed that the rate of cavitation is strain controlled and is independent of a range of strain rates extending across Region II into Region I of the stress–strain rate curve [1, 6, 7, 9]. For copper alloys with a high volume fraction of α-phase it has also been reported that the rate of cavitation is essentially independent of the superplastic deformation temperature [1, 7].

Much of the work on cavitation has been carried out using precision density measurements. It is difficult to analyse the data and get information on the nucleation and growth rates of cavities since cavities may nucleate continuously throughout plastic straining and also the nucleation rate may vary. In an attempt to reconcile the insensitivity of rate of cavitation to strain rate and temperature, and the possibility that cavities may nucleate continuously during superplastic straining, studies have been made on a fine grain

0022–2461/84 $03.00 + .12

α/β Cu–Zn–Ni–Mn alloy (nickel-silver) containing a high volume fraction of α-phase. The overall rate of cavitation has been examined as a function of strain, strain rate, temperature, using precision density measurements, while quantitative metallographic techniques have been used to determine the distribution of cavity sizes in the materials.

2. Experimental procedure

Tensile specimens of 10 mm gauge length and 5 mm gauge width were stamped from a batch of commercially available 1.5 mm thick sheet of microduplex nickel-silver alloy of nominal composition: Cu–28.1% Zn–15.0% Ni–13.3% Mn. The alloy, which has good microstructural stability, contained approximately 85% by volume of α-phase. The α-grain size was 2.2 μm (m.l.i.), and the β-phase size was $\sim 1\,\mu$m. Stress–strain rate characteristics and microstructural aspects of cavitation and of cavity growth in similar α/β nickel-silvers have been described previously [1, 7]. Tensile straining was carried out in air in a furnace attached to an Instron testing machine All tests were carried out using constant strain rates.

The volume of cavities in the gauge lengths of tensile specimens superplastically strained to predetermined extents was determined by hydrostatic weighing in ethyl iodide, with the undeformed gauge heads being used as density standards. Prior to density studies the gauge lengths and gauge heads were chemically cleaned in nitric acid.

Quantitative metallographic measurements of cavity size distributions were made on the metallographically polished gauge lengths of deformed specimens using a Quantimet Image Analyzing Computer. The observed distribution of cavity diameters was converted to a true size distribution using the Swartz–Saltykov analysis in which it was assumed that all the cavities were spherical [10].

It was noted that the number of cavities detected in the smallest size ranges examined, close to the limit of resolution of the Quantimet of $\sim 0.3\,\mu$m, was a sensitive function of the quality of surface preparation. For the largest cavity sizes where the number of sections in the prepared surface was small, i.e. $<10\,\text{mm}^{-2}$, small errors in counting could lead to apparently large but insignificant errors in the size distribution curves. As the number of cavities in the different size ranges varies widely, the results are presented as the logarithm of the number of cavities per mm^3 of diameter, d, against cavity diameter. As will be seen the total number of cavities per mm^3, N_v, in each distribution is dominated by those in the smallest size ranges.

3. Experimental results

3.1. Mechanical behaviour

Specimens were deformed to pre-determined elongations of 75%, 150%, and 225%, corresponding to strains of 0.56, 0.92 and 1.18, respectively, at various strain rates at temperatures in the range 470° C (743 K) to 560° C (833 K). The corresponding true stress–true strain data is summarized in Fig. 1 and, as can be seen, a wide range of stress levels was involved in the various tests. The deformation was carried out in Region II of the appropriate stress–strain curve, [1, 7] with the exception of the test at 743 K using a strain rate of $2.33 \times 10^{-3}\,\text{sec}^{-1}$. In the latter case deformation was carried out in Region III, resulting in the high stress level involved (Fig. 1). The fall in stress apparent for this specimen is the result of some necking due to the relatively low strain rate sensitivity associated with Region III.

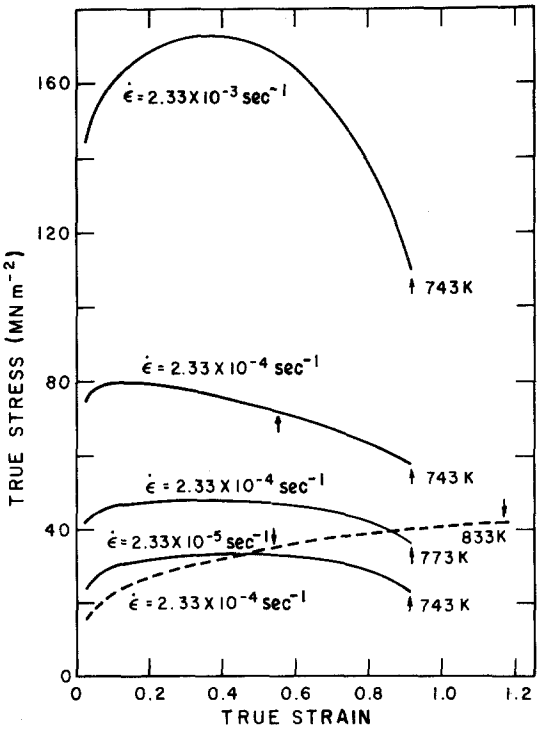

Figure 1 True stress–true strain curves corresponding to the superplastic tensile testing conditions.

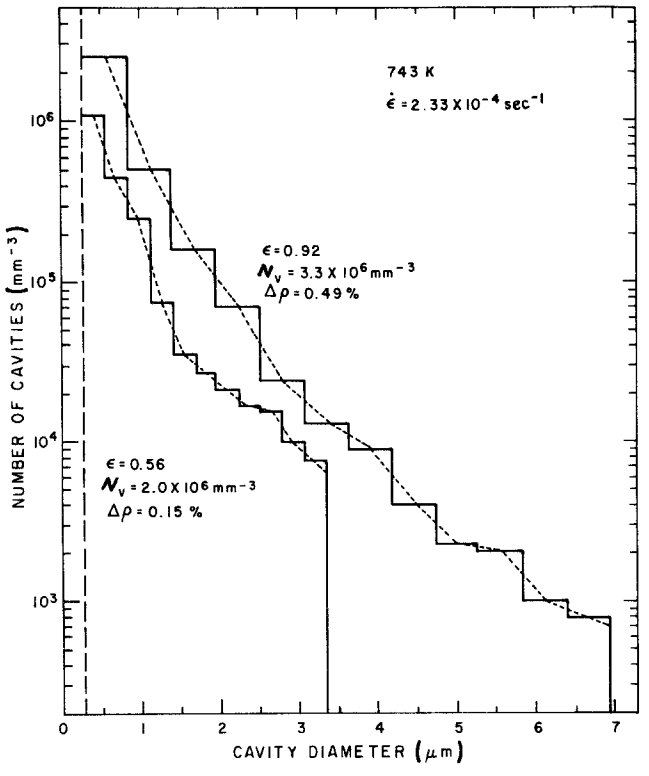

Figure 2 Cavity size distributions in specimens given superplastic strains of 0.56 and 0.92 at 743 K at a constant strain rate of $2.33 \times 10^{-4}\,sec^{-1}$.

3.2. Cavitation characteristics

Prior to examination of cavity size distributions in deformed specimens the overall levels of cavitation were obtained using density measurements. The total volume of cavities in the gauge length of each specimen was also obtained by point counting using the Quantimet. The two sets of measurements were in reasonable agreement and confirmed earlier measurements which showed that the volume of cavities in nickel-silvers was essentially independent of temperature of deformation and strain rate and was dependent only on the superplastic tensile strain [1, 7]. For superplastic true strains of 0.56, 0.92, and 1.18, the total volumes of voids were $0.15 \pm 0.01\%$, $0.49 \pm 0.11\%$ and $1.57 \pm 0.20\%$, respectively. The values obtained from density measurements tended to be slightly higher than those from point counting, probably because of the inability of the optical technique to resolve the smallest cavities.

3.3. Effect of strain

The effect of increasing superplastic strain on the distribution of cavity sizes is shown in Fig. 2. for specimens subjected to superplastic strains of 0.56 and 0.92, respectively, at 743 K at a constant strain rate of $2.33 \times 10^{-4}\,sec^{-1}$ ($1.4\%\,min^{-1}$), while Fig. 3 shows size distributions for strains of 0.56 and 1.18 at 833 K using the same strain rate. Fig. 4 shows micrographs of cavities in the polished specimens used to obtain the size distribution data shown in Fig. 3.

It can be seen from Figs. 2 and 3 that there is a range of cavity sizes for each strain and the spread of sizes and the total number of cavities in each size group tends to increase with increasing strain. For the specimen given a strain of 1.18 at 833 K (Fig. 3) the largest size group has been arbitrarly terminated at 6.95 μm, and the very small number of cavities with diameters greater than this size has been included within this group. Since the largest size group contained <10 cavities mm^{-2} before correcting for sectioning, this procedure is unlikely to introduce a significant error.

For the highest strain examined, $\epsilon = 1.18$, (Fig. 3), it can be seen that the numbers of cavities in the smallest size groups are less than those for the specimen subjected to a strain of 0.92 (Fig. 2), although under different conditions. Apart from problems associated with accurately recording the number of smaller cavities, the reasons for this are probably two-fold. Firstly, it is likely that the rate at which cavities become visible will fall-off with increasing strain as potential sites are acti-

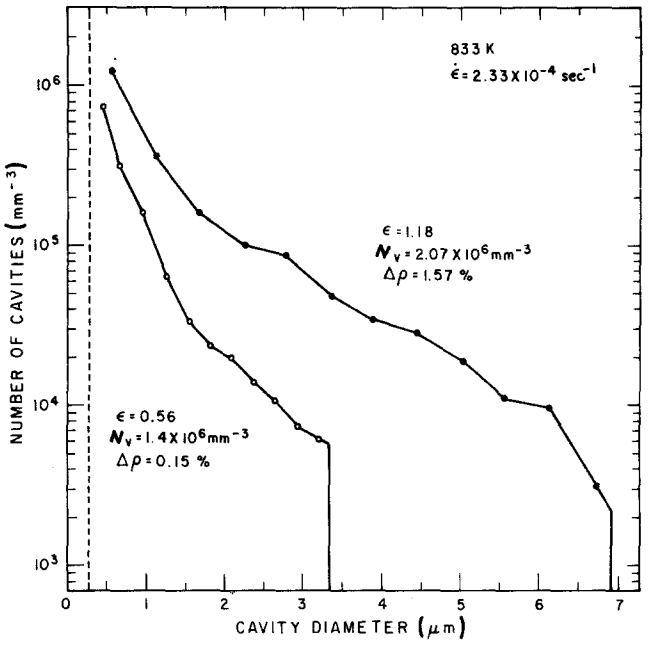

Figure 3 Cavity size distributions in specimens given superplastic strains of (a) 0.56 and (b) 1.19 at 833 K at a constant strain rate of 2.33×10^{-4} sec^{-1}.

vated and secondly, some cavity coalescence could lead to the loss of smaller cavities (Fig. 4b).

3.4. Effect of temperature

Cavity size distributions in specimens elongated to a strain of 0.56 at temperatures of 743 K and 833 K, respectively, at a constant strain rate of 2.33×10^{-4} sec^{-1} are shown in Fig. 5, while for the same strain rate Fig. 6 shows data obtained at 743 K and 773 K for specimens given a strain of 0.92.

It can be seen from Fig. 5 that the distributions of cavity sizes are similar although more cavities appear to have formed at the lower temperature. This could be related to the higher stress levels associated with the lower deformation temperature (Fig. 1), but as will be seen there is no obvious relationship throughout the results between applied stress and number of cavities observed. The higher number of cavities has had no effect on the density decrease and because of the potential problems associated with accurately measuring the number of cavities in the smallest and largest size ranges it is reasonable to suppose that the results show little significant difference.

For specimens strained to 0.92 at temperatures of 743 K and 773 K the distribution curves show either excellent or satisfactory agreement over the full range of cavity sizes involved (Fig. 6). The discrepancies at the larger cavity sizes could

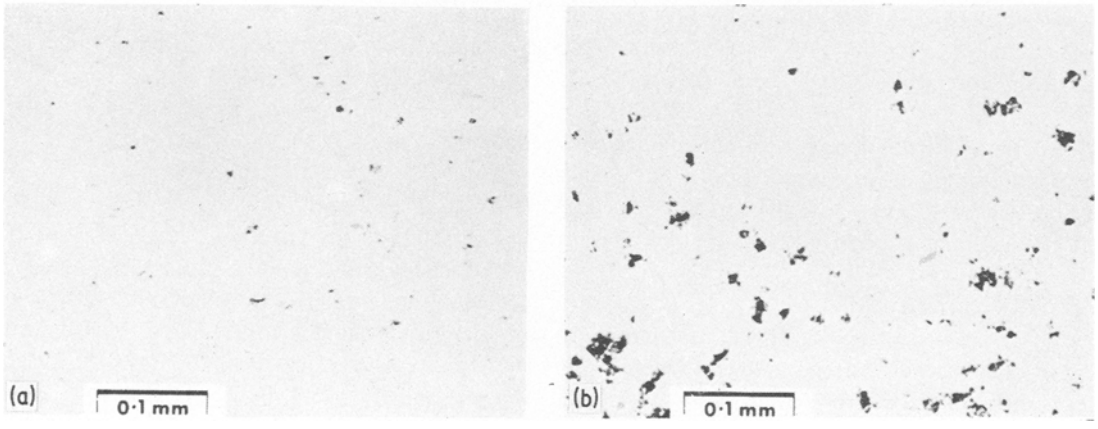

Figure 4 Cavities in polished specimens used to obtain the size distribution curves seen in Fig. 3. (a) $\epsilon = 0.56$; (b) $\epsilon = 1.18$.

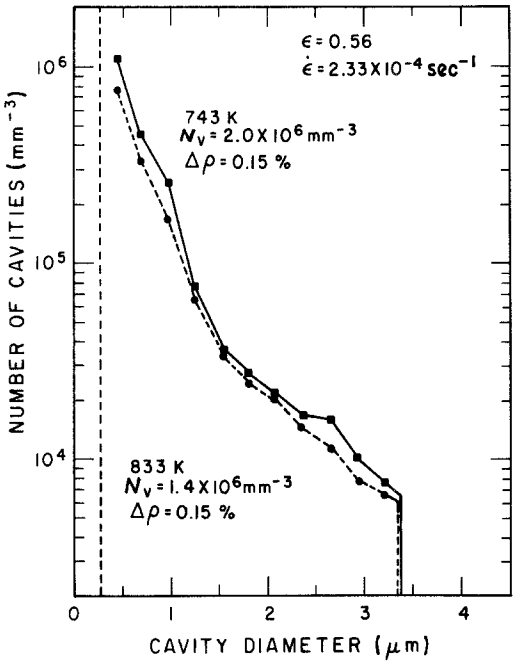

Figure 5 Cavity size distributions in specimens given a tensile strain of 0.56 at temperatures of 743 K and 833 K at a constant strain rate of $2.33 \times 10^{-4}\,sec^{-1}$.

be experimental in origin, or due to random cavity coalescence in the specimen strained at 773 K. The total number of cavities per mm^3, N_v, is very similar for the two specimens, primarily because of the good agreement between the large numbers of cavities in the smaller size ranges.

3.5. Effect of strain rate

The effect of strain rate on cavity-size distributions was examined for specimens superplastically deformed to a strain of 0.92 at a temperature of 743 K. The results are shown in Fig. 7 for strain rates of $2.33 \times 10^{-3}\,sec^{-1}$ (Region III), $2.33 \times 10^{-4}\,sec^{-1}$ and $2.33 \times 10^{-5}\,sec^{-1}$. Although the curves seem to show a systematic divergence at small cavity sizes, with the number of cavities increasing with decreasing strain rate, they show very good agreement for most of size ranges examined. Micrographs of the polished specimens are shown in Fig. 8.

The reason why the curves diverge at lower cavity sizes is not clear although some of the differences could be due to experimental scatter. For the highest strain rate, deformation is being carried out in Region III, and it can be seen from Fig. 1 that the associated stress levels are much higher (average of $150\,MN\,m^{-2}$) than those for deformation at the lower rates in Region II. It is possible that the initial microstructure may have been able to undergo significant grain boundary sliding in the earlier stages of deformation leading to cavity nucleation rates similar to those for

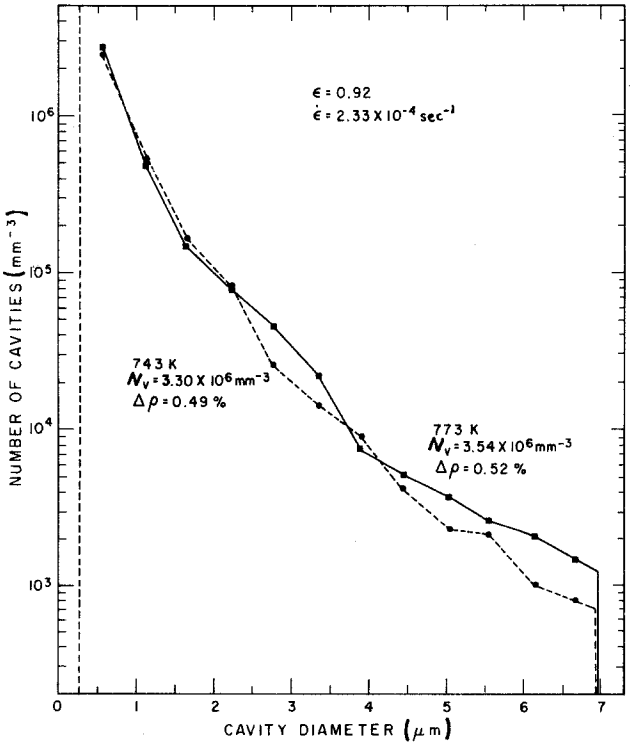

Figure 6 Cavity size distributions in specimens given a strain of 0.92 at 743 K and 773 K at a constant strain rate of $2.33 \times 10^{-4}\,sec^{-1}$.

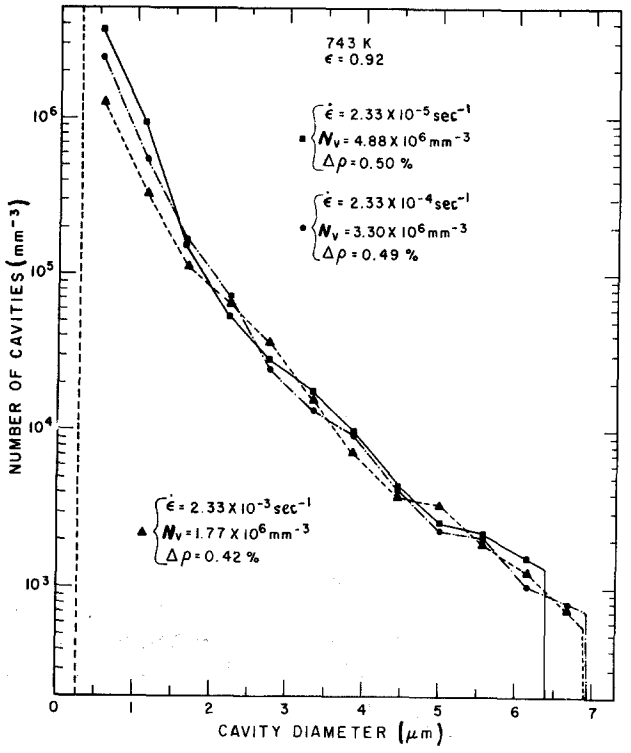

Figure 7 Cavity size distributions in specimens given a strain of 0.92 at 743 K at constant strain rates of $2.33 \times 10^{-3}\,sec^{-1}$, $2.33 \times 10^{-4}\,sec^{-1}$, and $2.33 \times 10^{-5}\,sec^{-1}$.

specimens deformed at lower rates in Region II. However, as the deformation proceeds dislocation creep will cause grain elongation and may reduce the ability of the grains to slide, and so the nucleation rate will drop off. For deformation in Region II at strain rates of $2.33 \times 10^{-4}\,sec^{-1}$ and $2.33 \times 10^{-5}\,sec^{-1}$, the smaller number of cavities is again associated with the higher flow stress levels ($68\,MN\,m^{-2}$ and $27\,MN\,m^{-2}$, respectively). The density changes in the latter specimens were 0.49

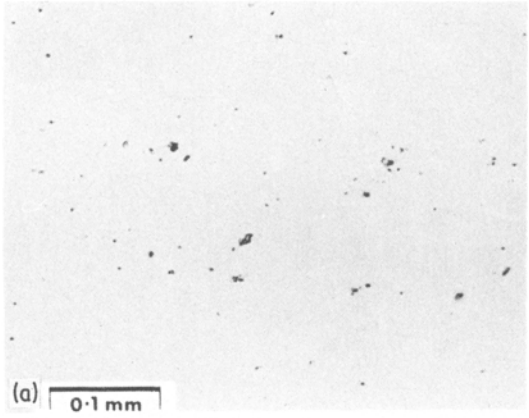

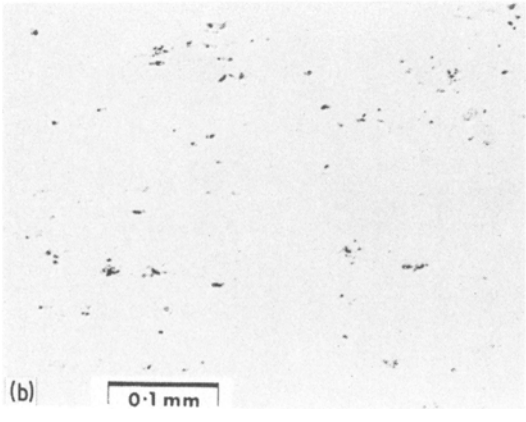

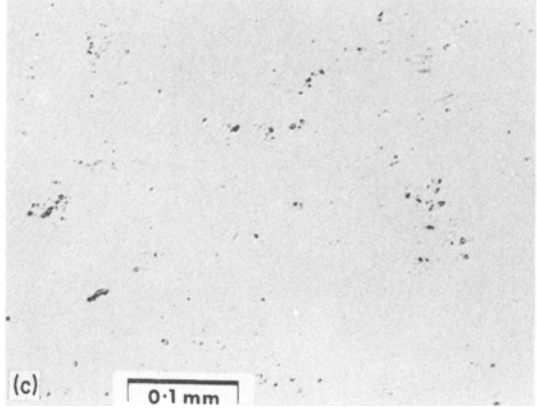

Figure 8 Cavities in polished specimens used to obtain size distribution data in Fig. 7. (a) $2.33 \times 10^{-3}\,sec^{-1}$; (b) $2.33 \times 10^{-4}\,sec^{-1}$; and (c) $2.33 \times 10^{-5}\,sec^{-1}$. $\epsilon = 0.92$.

and 0.50%, respectively, and it is suggested that there is little significant difference between the distribution curves.

4. Discussion

4.1. Cavity growth

The present results confirm earlier work and show that the volume of cavities produced in α/β nickel-silvers during superplastic tensile flow is dependent on strain, and independent of strain rate and temperature [1, 7]. The results also show that for each test condition there is a range of observable cavity sizes. The range of sizes and the numbers of cavities in the larger size groups increase with increasing strain. However, the number of cavities in each size group is determined only by strain, such that cavity size distribution curves for different temperatures and strain rates can be superimposed for the same strain.

The experimental results could be interpreted as showing that cavities nucleate continuously during superplastic flow and that the rates of nucleation and growth are determined primarily by plastic strain. However, the results do not in fact give information about cavity nucleation but about the size distribution of observable cavities all of which may have undergone appreciable growth. Stowell [11, 12] has questioned whether cavities nucleate during superplastic flow or whether they pre-exist and grow to a detectable size. There is evidence for commercial alloys that previous processing can lead to a distribution of defects [13–15]. This might be the case for the present alloy which is subjected to heavy deformation while in the α-phase condition, prior to a microduplex anneal at 480° C to recrystallize the α-phase and precipitate β.

A spherical cavity of critical dimensions located on a grain boundary, whether nucleated during superplastic flow or pre-existing, may grow by stress-directed vacancy diffusion or by plasticity control or by a combination of these proceses. The analysis of the former process by Raj and Ashby [16] leads to the relationship

$$\frac{dr}{d\epsilon} = \frac{\Omega D_B \delta}{2kT\dot{\epsilon}r^2}\left(\sigma - \frac{2\gamma}{r}\right)\frac{1}{\ln l/r - \frac{3}{4}} \qquad (1)$$

where r is cavity radius, ϵ is strain, $\dot{\epsilon}$ is strain rate, Ω is atomic volume, D_B is the grain boundary diffusion coefficient, δ is the grain boundary width, σ is the applied stress, γ is the surface energy of the cavity, k is Boltzmann's constant, T is the absolute temperature and l is the cavity spacing. For cavity growth by matrix deformation the relationship

$$\frac{dr}{d\epsilon} = r - \frac{3\gamma}{2\sigma} \qquad (2)$$

has been proposed [17].

Fig. 5 shows cavity distributions for deformation at 743 K and 833 K for a constant strain rate of $2.33 \times 10^{-4}\,\mathrm{sec}^{-1}$. From Fig. 1 it can be seen that the average flow stresses during deformation were 75 and 27 MN m^{-2}, respectively. Substitution of the above values of strain rate, temperature and stress into Equations 1 and 2 with $\Omega = 1.1 \times 10^{-29}$ m^{-3}, $D_B = 10^{-5}\exp(-103\,900/RT)\,\mathrm{m}^2\,\mathrm{sec}^{-1}$ [18], $\delta = 5.12 \times 10^{-10}$ m [16], $R = 8.314\,\mathrm{J\,K^{-1}\,mol^{-1}}$, $k = 1.38 \times 10^{-23}\,\mathrm{J\,K^{-1}}$, $\gamma = 1.2\,\mathrm{J\,m^{-2}}$ [19] leads to the relationships between cavity growth rate and cavity radius shown in Fig. 9. Equation 1 assumes a fixed array of pre-existing voids of constant spacing so an arbitrary value of $l = 15 \times 10^{-6}$ m has been used in the calculations. Although cavity spacing will change during deformation, previous work suggests that this value will not be much in error [7].

The curves in Fig. 9 predict that diffusional growth is dominant at small cavity sizes and that a transition occurs to plasticity controlled growth at larger sizes. These predictions are supported for α/β nickel-silvers by measurements of growth rates made for larger cavities, and by metallographic

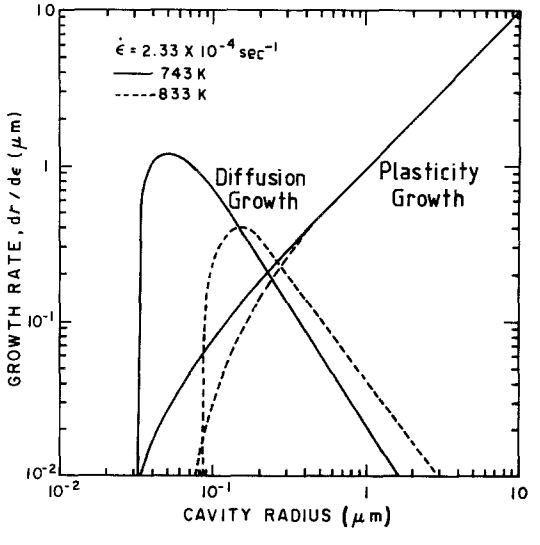

Figure 9 Predicted cavity growth rates for specimens given a tensile strain of 0.56 at temperatures of 743 K and 833 K at constant strain rate of $2.33 \times 10^{-4}\,\mathrm{sec}^{-1}$.

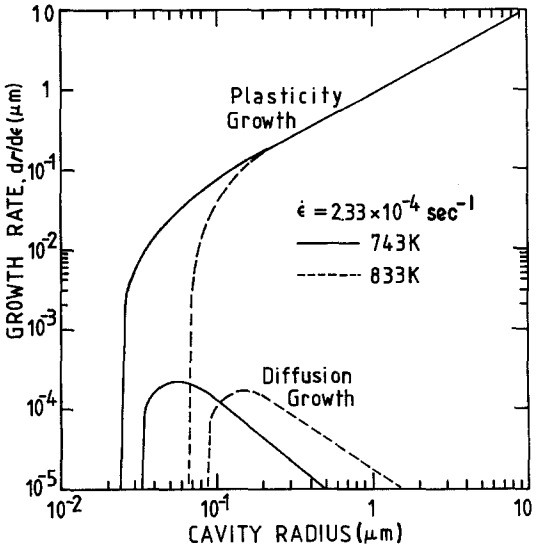

Figure 10 Predicted cavity growth rates for specimens given a tensile strain of 0.56 at temperatures of 743 K and 833 K at constant strain rate of $2.33 \times 10^{-4}\,sec^{-1}$. Recalculated using revised diffusion coefficient.

observations which show that diffusional growth leads to spherical cavities while plasticity controlled growth leads to eliptical cavities which are elongated in the direction of the applied stress, or to irregularly shaped cavities [7].

There is no grain boundary diffusion data for α/β nickel-silvers so the value of D_B used in the above calculations is that determined for copper. However, the authors have recently measured an activation energy of 157.2 kJ for α/β nickel-silver alloys during both tensile and compressive Region II superplastic flow over the range of temperatures of interest in the present work [20]. Using this activation energy the stress-directed vacancy diffusional growth rates have been recalculated and are shown in Fig. 10 with the plasticity controlled growth rates. The curves show that plasticity controlled growth is the dominant process for all stable nuclei. Similar results are obtained for the other conditions examined and have also been reported by Miller and Langdon [21] for superplastic zinc–aluminium. Although the calculations could be subject to error because it has been assumed that the pre-exponential term in the relationship for D_B is unaltered, they nevertheless provide strong evidence that cavity growth in α/β nickel-silvers is likely to be dominated by plastic deformation. Hence, the observation reported above that small cavities in superplastically deformed α/β nickel-silvers are usually spherical may be the result of surface diffusion, rather than diffusional growth.

4.2. Cavity nucleation

During superplastic flow incomplete accommodation of grain boundary sliding will lead to stress concentrations at grain boundary irregularities, triple points or/and second-phase particles, and to cavity nucleation. Continuous nucleation could result from the progressive involvement of new sliding surfaces or from grain-growth hardening. In the former case the rate of nucleation will eventually decrease as nucleation sites are used up. Following nucleation cavities will grow as described above.

Nucleation might be expected to occur relatively easily in microduplex α/β nickel-silvers because of the large volume fraction of α-phase they contain. If the alloy is analogous in its behaviour to α/β brass, then β will be the accommodating phase because of the relative ease of slip and the high diffusivity associated with this phase [6, 22]. According to Baudelet and Suery [22] all of the accommodation in α/β brasses occurs in the β-phase, and the α-phase behaves as a hard undeformable constituent. Hence, because of its inability to accommodate grain boundary sliding, nucleation of cavities would be expected to occur relatively easily particularly at second-phase particles on α/α boundaries.

Metallographic examination shows that cavities in α/β nickel-silvers are usually situated at α/β boundaries, [1, 7] but since the distance between β particles on α/α boundaries in relatively small, 1 to 2 μm, a cavity nucleated on an α/α boundary would only need to undergo very limited growth before impinging on a β particle.

Second-phase particles are likely to play a role in the nucleation process and SEM examination of specimens fractured in tension at room temperature following pre-cavitation at elevated temperature showed round particles approximately 1 μm in diameter located in cavities in the fracture face (Fig. 11). Subsequent microprobe analysis showed the particles to be sulphides [20].

Stowell, [11, 12] following earlier work by Harris [23] and Raj and Ashby [16], has given a relationship from which the critical strain rate, $\dot{\epsilon}_c$, below which cavity formation at a grain boundary particle of diameter, D, is inhibited by diffusive stress relaxation, can be estimated:

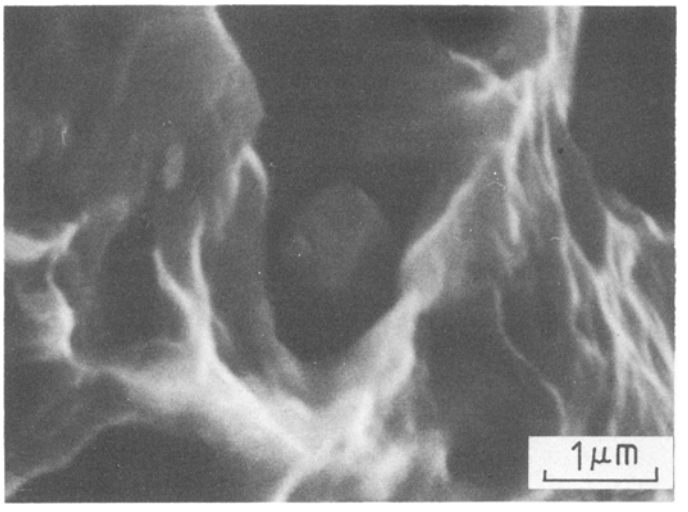

Figure 11 SEM micrograph showing a particle in a cavity in α/β nickel-silver alloy superplastically prestrained to 0.92 at 833 K and broken in tension at room temperature.

$$\epsilon_c \simeq \frac{11.5\sigma\Omega}{\alpha d D^2}\frac{D_B\delta}{kT} \quad (3)$$

where d is the grain diameter and α is the fraction of total strain carried by grain boundary sliding. Using D_B for copper and the values of Ω, δ and k given previously, with $\alpha = 0.5$, $d = 4\,\mu$m ($1.74 \times$ m.l.i.), $D = 1\,\mu$m, calculations of $\dot{\epsilon}_c$ have been made for the highest and lowest average stress levels involved in the present work: $\sigma = 150\,\text{MN m}^{-2}$ at 743 K; $\sigma = 27\,\text{MN m}^{-2}$ at 833 K. For both of these conditions it was predicted that particles greater than 1 μm would nucleate cavities during superplastic flow at a strain rate of $\sim 3 \times 10^{-4}\,\text{sec}^{-1}$.

If $\dot{\epsilon}_c$ is recalculated using the activation energy measured by the authors [20], then $\dot{\epsilon}_c$ becomes 10^{-7} to $10^{-8}\,\text{sec}^{-1}$, which is more than three order of magnitude less than the figure previously obtained. Although, as indicated earlier, the recalculated figure could be subject to error, it is likely that cavity nucleation at second-phase particles located on α/α boundaries can occur readily during superplastic flow under the conditions investigated. The observation of sulphides in cavities formed during superplastic flow, Fig. 11, is consistent with nucleation of these cavities by second-phase particles.

In this work on a superplastic aluminium alloy Ghosh [24] developed a cavitation model based on dynamic nucleation and growth of cavities. Nucleation sites were provided by second-phase particles on grain boundaries. It was assumed that nucleation was diffusion assisted and when the flow stress exceeded a value given by $\sigma = 2\gamma/r$, where γ is the surface free energy, cavities nucleated on particles of radius, r. Grain-growth leads to strain hardening and to progressive nucleation of new cavities as the nucleation stress for smaller cavities is reached. Once nucleated, grain boundary cavities grow by plastic flow of the surrounding matrix. The Ghosh model predicts that the number of cavities nucleated and the void volume will increase with increasing strain rate and decreasing temperature, both of which are associated with increasing flow stress. In the present work the void volume and the number of optically visible cavities were not affected by strain rate or temperature, and were independent of both the level of flow stress and whether the stress was rising or falling during the test (Fig. 1). In general the stress levels were much higher than those involved in the aluminium alloy studied by Ghosh.

4.3. Evidence for pre-existing voids

Stowell [25] has developed a model for cavitation in which it is assumed that (i) all voids pre-exist at zero strain, (ii) all voids are the same size and (iii) cavity growth is plasticity controlled. The analysis predicts that the volume fraction of cavities, ϕ, should have an exponential dependence on strain, ϵ, according to the relationship

$$\phi = \phi_0 \ln(\eta\epsilon) \quad (4)$$

where ϕ_0 is the level of cavitation at zero strain and η is a parameter which usually has a value in the range 2 to 3, but is dependent on the alloy, and on strain rate, temperature and grain size. Despite the fact that a range of cavity sizes is usually encountered, much of the available data can be fitted to the above equation.

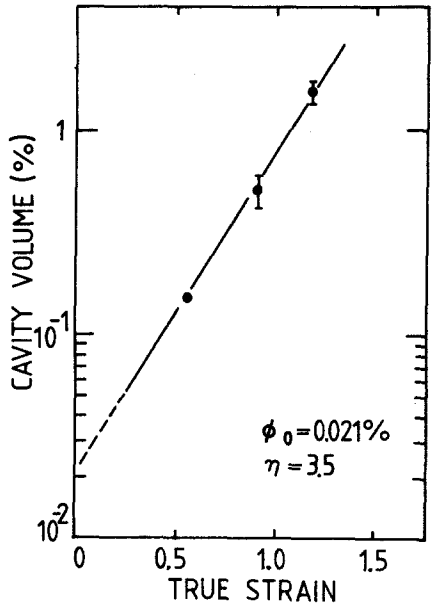

Figure 12 Variation of measured cavitation level with strain for microduplex α/β nickel-silver alloy.

The present cavitation data is plotted in Fig. 12 and gives values of $\phi_0 = 0.021\%$ and $\eta = 3.55$. The latter value is higher than $\eta = 2.2$ and 2.5 obtained from earlier cavitation data for microduplex α/β nickel-silvers, while the value of ϕ_0 is appreciably smaller than previous values of 0.2% and 0.33%. The small value of ϕ_0 suggests that the volume of pre-existing voids in the present material is much less than for the alloys previously examined, possibly due to a higher purity material and/or a different thermomechanical processing procedure. However, the value of ϕ_0 was consistent with the generally lower levels of cavitation in the present material compared with those examined earlier.

In the Stowell model the value of ϕ_0 depends on how many of the pre-existing cavities are stable under superplastic testing conditions. It was assumed, following Hancock [17], that voids with a critical radius $> 3\gamma/2\sigma$, where γ is the surface energy, would grow under the action of the applied stress, σ, while cavities smaller than this would shrink. If the strain rate were increased or the temperature decreased the stress would increase and the critical void size would decrease, giving a larger effective value of ϕ_0. The reverse would be true for decreasing strain rate or increasing temperature. In the present work the value of ϕ_0 is independent of strain rate and temperature, and hence stress. However, for the range of average stresses involved the critical void nuclei would be expected to have diameters in the range 0.02 to 0.13 μm ($3\gamma/\sigma$). The values shown in Fig. 10 correspond to diameters of 0.05 and 0.13 μm.

Stowell [11] has rewritten Equation 4 to give

$$D_\epsilon = D_0 \exp\left(\frac{\eta\epsilon}{3}\right) \quad (5)$$

where D_ϵ is the cavity diameter after strain ϵ, and D_0 is the initial cavity diamter. For deformation at 743 K at $2.33 \times 10^{-4}\,\text{sec}^{-1}$ the dimensions of the largest cavities observed after a strain of 0.56 (75 per cent elongation) were $\sim 3.5\,\mu$m (Fig. 5). To produce a cavity of this size at this strain would require a cavity of initial diameter $\sim 1.8\,\mu$m. Following nucleation, even if a cavity was able to grow relatively rapidly by diffusion in its early stages it is apparent that the largest observable cavities have grown from pre-existing voids. The cavity distribution data for strains of 0.92 and 1.18 also predicts initial cavity diameters of $\sim 2\,\mu$m.

The smallest size of cavity which would be optically resolvable ($\sim 0.4\,\mu$m – average dimensions of smallest size group measured) would grow from a cavity of inital diameter $\sim 0.2\,\mu$m. Hence, any void nucleus of diameter $< 0.2\,\mu$m could not grow to a size where it would become optically resolvable after a strain of 0.56. A cavity of critical dimensions ($\sim 0.05\,\mu$m for the deformation conditions under discussion, Fig. 10.) would be predicted to achieve a diameter of $\sim 0.10\,\mu$m after a strain of 0.56, which is well below the limit of optical resolution. For the critical cavity to achieve resolvable dimensions would require a strain of 1.76 (480% elongation). Similar conclusions could be drawn for the other deformation conditions examined.

4.4. Independence of cavitation on strain rate and temperature

It is apparent for the present alloy that some cavities must pre-exist as flaws in the microstructure and it is also highly likely that during superplastic flow cavity nucleation will occur, particularly on second-phase particles. Early in a given test a range of initial cavity diameters will exist extending from $\sim 2\,\mu$m down to a critical size dependent on stress. Independent of whether the cavities pre-exist or are nucleated, their growth is plasticity dominated (Equation 5). Although cavitation is independent of strain rate and tem-

perature, these parameters will influence the flow stress.

During straining, only those cavities with initial dimensions which exceed a certain value, determined by strain, will grow to an optically resolvable size. For a given strain there will be more non-resolvable cavities in a specimen deformed at a high stress than at a low stress. However, the overall decrease in density in the two specimens will be similar because the additional cavities associated with the higher stress will be in the very small size range and will have no significant effect on density change. The bulk of the density decrease will be due to optically visible cavities. If nucleation is continuous during straining due to an increase in stress or to the involvement of new sliding surfaces, the cavities introduced could not grow sufficiently to effect a change of density.

In the specimen deformed to a strain of 0.56 (Figs. 5 and 10) the initial cavity sizes will extend from $\sim 2\,\mu m$ down to critical diameters of $0.13\,\mu m$ for the low stress and $0.05\,\mu m$ for the higher stress. A density differential would be expected due to the existence and growth of cavities with diameters initially in the size range 0.05 to $0.13\,\mu m$, in the specimen subjected to higher stress. However, after growth these cavities still have dimensions well below the limit of optical resolution and because of their small sizes have little effect on density. An estimate of the number of cavities that exist in the non-resolvable size range of the specimen given a true strain of 0.56 at 743 K can be obtained by extrapolating the data for the smaller resolvable size groups (Figs. 2 and 5). The extrapolation predicts $\sim 3 \times 10^6$ cavities per mm^3 in the size range 0 to $0.278\,\mu m$. Assuming a mean cavity diameter of $0.14\,\mu m$ then the non-resolvable size group is calculated to reduce the density by approximately 0.0004 per cent, which is an insignificant decrease.

5. Conclusions

1. A microduplex α/β copper–zinc–nickel–manganese alloy containing approximately 85 per cent volume of α-phase underwent cavitation during superplastic tensile flow. The level of cavitation increased as the strain was increased but was essentially independent of strain rate and temperature.

2. The number of cavities that become optically visible increased throughout straining, but the rate at which they became visible decreased at higher strain levels.

3. For each strain a range of cavity sizes was observed, and the range of sizes and the numbers of cavities in the larger size groups increased with increasing superplastic strain.

4. The number of cavities in each size group was determined by strain and cavity size distribution curves for different temperatures and strain rates superimposed for a given strain.

5. There was evidence that cavities grew from pre-existing flaws and were also nucleated, particularly at grain boundary second-phase particles during superplastic flow.

6. Growth for all cavity sizes was dominated by matrix plastic flow.

7. The apparent insensitivity of cavity volume and cavity size distribution to strain rate and temperature, and hence stress, reflects the resolution of the density and metallographic techniques. Although higher stresses will lead to a wider range of initial cavity sizes primarily by lowering the critical nucleus size, cavities at the lower end of the size range will not grow sufficiently large to become optically resolvable or to produce a density differential compared with a specimen deformed to the same extent at a lower stress.

Acknowledgements

The authors are grateful to Inco Europe Limited for the supply of materials. The work was carried in the University of California, Davis, California and in the University of Manchester/UMIST. The authors are grateful to NSF (Grant No NSF-DMR-7727724) and SERC, respectively, for finanical support.

References

1. D. W. LIVESEY and N. RIDLEY, *Met. Trans.* **9A** (1978) 519.
2. C. W. HUMPHRIES and N. RIDLEY, *J. Mater. Sci.* **13** (1978) 2477.
3. T. CHANDRA, J. J. JONAS and D. M. R. TAPLIN, *J. Aust. Inst. Metals* **20** (1975) 220.
4. S.-A. SCHEI and T. G. LANGDON, *J. Mater. Sci.* **13** (1978) 1084.
5. J. BELZUNCE and M. SUERY, *Scripta Metall.* **15** (1981) 895.
6. W. J. D. PATTERSON and N. RIDLEY, *J. Mater. Sci.* **16** (1981) 457.
7. D. W. LIVESEY and N. RIDLEY, *Met. Trans.* **13A** (1982) 1619.
8. W. J. CLEGG, J. A. ROOUM and A. K. MUKHERJEE, in Proceedings of the 6th International Conference on Strength of Metals and Alloys, Melbourne,

Australia (1982) p. 689.
9. C. H. CACERES and D. S. WILKINSON, in "Superplastic Forming of Structural Alloys", edited by N. E. Paton and C. H. Hamilton, (The Metallurgical Society of AIME, Warrendale, 1982) p. 408.
10. E. E. UNDERWOOD, "Quantitative Stereology" (Adison-Wesley, New York, 1970) p. 119.
11. M. J. STOWELL, in "Superplastic Forming of Structural Alloys", edited by N. E. Paton and C. H. Hamilton (The Metallurgical Society of AIME, Warrendale, 1982) p. 321.
12. M. J. STOWELL, *Met Sci.* **17** (1983) 1.
13. S. H. GOODS and L. M. BROWN, *Acta Metall.* **27** (1979) 1.
14. I. W. CHEN and A. S. ARGON, *ibid.* **29** (1981) 1321.
15. P. G. SHEWMON, H. LOPEZ and T. A. PARTHASARATHY, *Scripta Metall.* **17** (1983) 39.
16. R. RAJ and M. F. ASHBY, *Acta Metall.* **23** (1975) 653.
17. J. W. HANCOCK, *Met. Sci.* **10** (1976) 319.
18. M. F. ASHBY, *Acta Metall.* **20** (1972) 887.
19. H. JONES, *Met. Sci.* **5** (1971) 15.
20. N. RIDLEY, D. W. LIVESEY and A. K. MUKHERJEE, to be published.
21. D. A. MILLER and T. G. LANGDON, *Met. Trans.* **10A** (1979) 1869.
22. M. SUERY and B. BAUDELET, *Phil. Mag.* **41A** (1980) 41.
23. J. E. HARRIS, *Trans. AIME* **233** (1965) 1509.
24. A. K. GHOSH, in "Deformation of Polycrystals: Mechanisms and Microstructures", edited by H. Hanson, A. Horsewell, T. Leffers and H. Lilholt (Riso National Laboratory, Roskilde, Denmark, 1981) p. 227.
25. M. J. STOWELL, *Met. Sci.* **14** (1980) 267.

Received 7 July
and accepted 28 July 1983